HHS Public Access

Author manuscript

Acta Biomater. Author manuscript; available in PMC 2018 January 15.

Published in final edited form as:

Acta Biomater. 2017 January 15; 48: 186–194. doi:10.1016/j.actbio.2016.10.023.

Effect of anticoagulants on the protein corona-induced reduced drug carrier adhesion efficiency in human blood flows

Daniel J. Sobczynski[a] and **Omolola Eniola-Adefeso**[a,b,*]

[a]Department of Chemical Engineering, University of Michigan, Ann Arbor, MI, 48109, United States of America

[b]Department of Biomedical Engineering, University of Michigan, Ann Arbor, MI, 28109, United States of America

Abstract

Plasma proteins rapidly coat the surfaces of particulate drug carriers to form a protein corona upon their injection into the bloodstream. The high presence of immunoglobulins in the corona formed on poly(lactic-co-glycolic acid) (PLGA) vascular-targeted carrier (VTC) surfaces was recently shown to negatively impact their adhesion to activated endothelial cells (aECs) *in vitro.* Here, we characterized the influence of anticoagulants, or their absence, on the binding efficiency of VTCs of various materials via modulation of their protein corona. Specifically, we evaluated the adhesion of PLGA, poly(lactic acid) (PLA), polycaprolactone (PCL), silica, and polystyrene VTCs to aECs in heparinized, citrated, and non-anticoagulated (serum and whole) blood flows relative to buffer control. Particle adhesion is substantially reduced in non-anticoagulated blood flows regardless of the material type while only moderate to minimal reduction is observed for VTCs in anticoagulant-containing blood flow depending on the anticoagulant and material type. The substantial reduction in VTC adhesion in blood flows was linked to a high presence of immunoglobulin-sized proteins in the VTC corona via SDS-PAGE analysis. Of all the materials evaluated, PLGA was the most sensitive to plasma protein effects while PCL was the most resistant, suggesting particle hydrophobicity is a critical component of the observed negative plasma protein effects. Overall, this work demonstrates that anticoagulant positively alters the effect of plasma proteins in prescribing VTC adhesion to aECs in human blood flow, which has implication in the use of *in vitro* blood flow assays for functional evaluation of VTCs for *in vivo* use.

Graphical Abstract

*Corresponding author at: Department of Chemical Engineering, University of Michigan, 2800 Plymouth Road, NCRC B28-G046W, Ann Arbor, MI 48109, United States of America. lolaa@umich.edu (O. Eniola-Adefeso); Tel:(+1)734.936.0856; Fax: 734.764.7453.

6. Disclosures

The authors have no conflicts of interest.

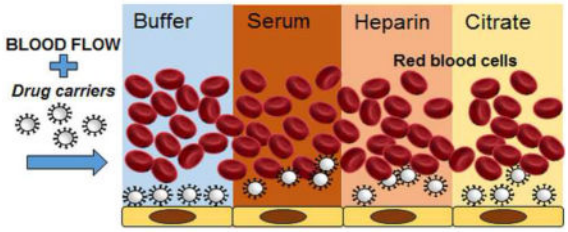

Keywords

Nanoparticles; Protein Corona; Serum; Plasma; Blood Flow; Vascular-Targeting

1. Introduction

Vascular-targeted drug delivery has long been explored for use as an efficient and non-invasive alternative to current treatments for a variety of diseases, most notably, cancer [1,2]. Vascular targeting offers great potential to reduce side effects of non-specific cytotoxic drugs and increase overall therapeutic potency. However, several challenges still remain for this approach. Optimal VTC efficacy hinges on successful localization and adhesion of carriers to the vascular wall at the target site. Thus, VTC characteristics, including size, shape and surface characteristics that result in low VTC localization or adhesion to the vascular wall will undoubtedly hinder any potential benefit of this approach. Previously, rapid formation of a unique protein corona on poly(lactic-co-glycolic) acid (PLGA)-based VTCs was shown to drastically reduce their adhesion efficiency to inflamed endothelium in human blood flow; however, this effect was largely non-existent for polystyrene (PS), silica (Si), and titanium dioxide (TiO_2) particles [3–5]. This plasma protein effect was linked to a unique, large presence of immunoglobulin sized (~150 kDa) proteins in the PLGA corona [3].

Although the protein corona is known to influence many processes such as targeted nanoparticle (NP) uptake [6] and VTC adhesion to the vascular wall [3,5], very limited studies have explored the influence of suspending fluid (i.e. plasma anticoagulant or its absence) in these processes. Serum (no anticoagulant) and anticoagulated plasma are both routinely used to assess NP-protein interaction for drug delivery applications, yet these mediums have their own unique protein composition, which can influence the type of proteins that adsorb on particle surfaces [6–11]. Specifically, concentrations of chemokines, complement factors, and apolipoproteins have been reported to increase in serum relative to plasma [7,12]. On the contrary, the concentration of coagulation proteins, such as fibrinogen, is significantly reduced in serum relative to anticoagulated plasma, and overall, serum tends to have a slightly lower total protein content than plasma [13]. Likely a result of these composition differences, unique particle protein coronae have been reported between serum and plasma exposed particles, resulting in differential cellular interactions [14,15]. Similarly, the composition of proteins in plasma has been shown to significantly change with the choice of anticoagulant, i.e. citrate versus heparin [8,12]. Heparin binds to a number of proteins commonly called “heparin-binding proteins”, including fibronectin, apolipoproteins, complement C3 and C4b, and antithrombin [16], and this binding process can affect the activity and plasma concentration of these proteins [17,18]. Indeed, Kim et al.

reported an increased concentration of Apo-AI and α2-macroglobulin in heparin relative to citrated plasma [12]. Furthermore, Schöttler et al. reported corona differences (increased fibrinogen and decreased vitronectin) observed between citrate relative to heparin exposed particles [14]. Despite this knowledge of differences in protein composition of serum and plasma or of different anticoagulants, the role of these differences in protein corona formation and the potential role in prescribing VTC adhesion to the vascular wall remain unknown.

In this work, we evaluate how protein adsorption and, subsequently, particle adhesion is affected by the characteristics of the suspending blood fluid and particle material type. Specifically, we employed viscous buffer, acid-citrate-dextrose (ACD) treated plasma, heparinized plasma, serum and anticoagulant-free whole blood as mediums for the flow adhesion of ~500 nm PLGA, poly(lactic acid) (PLA), polycaprolactone (PCL), PS and Si particles to activated human umbilical vein endothelial cells (HUVEC) in a parallel plate flow chamber (PPFC). A particle's material type has been identified to cause substantial differences in the composition of proteins present in the particle's surface adsorbed corona and thus represents a critical parameter to explore in this study [19,20]. Particles made from PLGA, PLA and PCL polymers were used in this study since they are biodegradable polyesters typically used in the construction of VTCs. PS and Si serve as control materials in our assays to allow comparison to existing literature. Both citrated (ACD) and heparinized whole bloods are explored as flow medium, as these are commonly used anticoagulants for blood draw that also act by different mechanisms [8]. ACD chelates calcium ions, thus preventing the clotting process, whereas heparin acts by binding to antithrombin III, causing inactivation of thrombin [12]. These differences in mechanism of action between ACD and heparin can have profound impacts on the overall plasma composition [7,12,18,21]. We investigate differences in particle binding between serum and anticoagulated plasma to determine if the absence of clotting factors/proteins, as is the case for serum (anticoagulant free), impacts particle adhesion from flow based on the known significant changes in the protein corona formed onto VTCs between these two mediums [7,22]. Anticoagulant free whole blood is used here in an attempt to best resemble particle interaction *in vivo* in humans. We then probed whether any observed corona-induced adhesion reduction is mitigated by increased copies of targeting ligand on the particle surface for the different materials, as observed previously with PLGA microparticles [3]. Non-pegylated (non-PEG) particles are employed throughout this study to highlight the impact of material type in any observed corona-induced effects, which can shed light on the extent of surface modification required for VTCs of different materials to successfully reduce or alter plasma protein adsorption.

2. Materials and methods

2.1 Particle size and concentration characterization

PLGA, PLA, and PCL carboxylated 500 nm particles were obtained from Phosphorex, Inc. (Hopkinton, MA). The VTC particle concentration was obtained by manual counting on a hemacytometer (Hausser-Scientific). Non-fluorescent particles were used to limit any effect of a fluorescent dye on VTC-protein interaction. Particles were rendered fluorescent after

the plasma/serum/VB incubation and prior to use in flow assays. Si and PS green fluorescent particles were purchased from Corpuscular (Cold Spring, NY) and Polysciences, Inc. (Warrington, PA), respectively. VTC size was measured by dynamic light scattering (DLS) using a Malvern Zetasizer instrument. Carboxylated stocks were dispersed in PBS++, with 1% bovine serum albumin (BSA) and then washed with 50 mM PBS prior to making the DLS measurement. Carboxylated biodegradable PLGA, PLA, and PCL particles were soaked in 50 mM MES at pH 7 (for PCL, pH ~5) for ≥ 20 hr prior to DLS measurement which corresponds to the time required for NeutrAvidin conjugation to these particles. VTC diameters ranged from ~400–700 nm as listed in Table 1. Table 2 lists the average sLe^a ligand site density of the various VTC materials.

2.2 Surface ligand conjugation

Particle stocks were first conjugated with NeutrAvidin via covalent carbodiimide chemistry followed by linkage to biotinylated sialyl-Lewis^a (sLe^a) (Glycotech Corporation). The coupling of NeutrAvidin has been described elsewhere [23]. Briefly, an approximate particle surface area of 9.1×10^9 μm^2 mL^{-1} of conjugation volume was used. Particle concentration was determined by manual count of a known volume of particle solution using a hemocytometer. The conjugation volume consisted of equal parts NeutrAvidin (5 mg mL^{-1}) and *N*-Ethyl-*N*′-(3-dimethylaminopropyl) carbodiimide hydrochloride (EDAC) (Sigma) (75 mg mL^{-1}) dissolved in 50 mM 2-(*N*-morpholino)ethanesulfonic acid (MES) buffer. VTCs were first incubated with 5 mg mL^{-1} NeutrAvidin for 15 min, followed by addition of an equal volume of EDAC at 75 mg mL^{-1}. 1 M sodium hydroxide (NaOH) was added (~47 μL mL^{-1} conjugation volume) to pH the solution to ~7.4 and allowed to rotate on an end-to-end rotator for ~20 hr. Following the 20 hr incubation step, ~7.5 mg glycine mL^{-1} conjugation volume was added to stop the crosslinking reaction and allowed to incubate for 30 min. This NeutrAvidin attachment protocol is expected to yield a consistent density of avidin across material types – a density of ~ 1.1 x 10^5 and 9.7 x 10^4 avidin μm^{-2} was achieved for PLGA and PS, respectively. Conjugated VTCs were washed and re-suspended in 1 mL of 50 mM phosphate buffered saline (PBS).

Attachment of the targeting ligand was performed by suspending NeutrAvidin coated particles in 100 μL of biotinylated sLe^a (diluted in PBS with calcium and magnesium (PBS++) with 1% BSA) at concentrations ranging from 0.4 to 10 μg mL^{-1}. Surface area to volume ratio of the various VTCs was varied to achieve the desired ligand site density. NeutrAvidin-coated particles were allowed to rotate in the targeting ligand solutions for 45 min, and then washed three times with PBS++ 1% BSA buffer and suspended in a final volume of 1 mL. The zeta potentials for sLe^a particles exposed to plasma or serum were obtained using the Malvern Zetasizer instrument.

2.3 Quantification of ligand density

Targeting ligand density was quantified via flow cytometry using an Attune flow cytometer (Applied Biosystems) as described elsewhere [23]. For quantifying sLe^a density, 1×10^6 particles were incubated for 20 min in a 1:10 solution (100 μL volume) of anti-CLA-PE (Miltenyi Biotec). Following the incubation step, VTCs were washed three times with PBS++ with 1% BSA buffer and suspended in a final volume of 1 mL. Rat-IgM-PE (Fisher

Scientific) was used as the isotype control. Quantification of the number of ligand sites on the particle surface was achieved via use of Quantum R-PE MESF calibration beads (Bangs Laboratories). Specifically, the amount of fluorescent molecules was correlated to fluorescence intensity via a calibration curve. The number of sites was then determined based on the differences in the median fluorescence intensity between the anti-CLA-PE stained and Rat-IgM-PE stained particles. To assist in gating and visualization of non-fluorescent 500 nm particles during flow cytometry, sLe^a-coated particles were stained with biotin-FITC prior to sample testing.

2.4 HUVEC culture

Human umbilical vein endothelial cells (HUVECs) were obtained via a commonly used collagenase perfusion method [24]. Umbilical cords were generously donated by the U of M hospital under a Medical School Internal Review Board (IRB-MED) approved human tissue transfer protocol (HUM00026898). The protocol is exempt from informed consent per federal exemption category #4 of the 45 CFR 46.101.(b). HUVECs isolated from the umbilical cords were pooled and grown in tissue culture using T-75 flasks pre-coated with 0.2 wt% gelatin. Preparation of HUVEC coated coverslips for flow chamber assays is described elsewhere [24,25]. HUVEC monolayers were activated with 1 ng mL^{-1} interleukin 1-beta (IL1-β) for 4 hrs prior to performing the flow experiment to facilitate binding of sLe^a-coated particles via upregulation of human E-selectin.

2.5 Blood preparation

Blood was obtained from healthy human donors according to a protocol approved by the University of Michigan Internal Review Board. Informed, written consent was obtained from all subjects prior to blood collection. Anticoagulant solutions were added to blood at a ratio of 7 mL to 50 mL of blood. To obtain serum, blood without any additive was allowed to sit upright in a 50 mL conical tube for at least 2 hr, and then centrifuged at 2000g for 10 min at 4°C. For plasma collection, ACD or heparinized whole blood (WB) was centrifuged at 2250g for 20 min at 4°C. An additional spin at 6797g for 5 min was employed to remove residual white blood cells and platelets from plasma. To determine the hematocrit, whole blood was centrifuged at 2250g for 20 min at 4°C and the ratio of RBC volume to total blood volume was taken as the hematocrit value. Suspension of washed RBCs in viscous buffer (RBCs-in-VB), a buffer solution with viscosity matching that of human plasma and consisted of PBS++ with 1 wt% BSA and 1.4 wt% dextran, is used here as control. To prepare reconstituted blood assays (e.g. RBCs-in-VB, RBCs-in-Serum), RBCs from ACD WB were washed 3 times with PBS−− via centrifugation at 1000g for 30 min. A final wash was performed at 2250g for 20 min, and VB or serum was added to the RBC pellet to achieve a matching hematocrit to that obtained with ACD whole blood. An average hematocrit of 44 ± 1 (S.E.)% was used for all assays.

2.6 Parallel plate flow chamber (PPFC) assay

Flow adhesion assays were performed using a Nikon TE 2000-S inverted microscope fitted with a digital camera. The microscope incubator was heated to ~37°C prior to the experiment. A circular parallel plate flow chamber (Glycotech Corporation; Supplement Figure 1) containing a straight rectangular channel was used for all flow assays as previously

described elsewhere [3,23–25]. Briefly, for each trial, an activated coverslip containing a monolayer of HUVEC was vacuum-sealed to the bottom of the flow chamber deck. The outlet of the flow chamber is connected to a syringe pump, which controls the flow rate. Vascular-targeted particles were incubated for 5 min in buffer, serum, or plasma, mixed and then added to the flow medium (blood, RBCs-in-Serum, or RBCs-in-VB) at a concentration of 1×10^6 particles mL^{-1} and the mixture then added to a syringe connected to the flow chamber inlet. The duration of each flow assay was 5 min at a shear rate of 200 s^{-1}. After the flow experiment, the amount of bound VTCs along the channel width, at a fixed position from the channel entrance, was obtained by fluorescent imaging, which allowed for quantification of singlet bound particles. Particle stocks were sonicated briefly prior to use in assays to minimize particle aggregation. For the biodegradable VTCs (PLGA, PLA, PCL), particle fluorescence was achieved by labeling particles using biotin-PE antibody (added 3 μL of 1 mg mL^{-1} biotin-PE solution) after exposure to plasma, serum, or VB (300 μL) for 5 min to set the corona prior to labeling. For anticoagulant-free (ACF) WB assays, biotin-PE stained biodegradable VTCs stored in flow buffer were added to ACF blood and immediately used in assays. Particles were not exposed to ACF plasma prior to the ACF WB assay as ACF WB had to be drawn and used immediately before substantial clotting.

2.7 SDS-PAGE

SDS-PAGE was performed using 4–20% precast gels from Bio-Rad laboratories. sLe^a VTCs were exposed to plasma (ACD or heparinized), serum, ACF plasma or VB for a total of 10 min – comprised of a 5 min incubation step followed by a 5 min centrifugation step to remove the soaked particles from the incubation media – similar to the preparation for the flow assay. For the ACF plasma assay, ACF WB was spun immediately after venipuncture at 2250g for 10 min followed by a spin at 8000 RPM for 5 min. After 3 min of particle exposure to ACF plasma, 140 μL mL^{-1} ACD was added to ACF plasma-suspended particles (referred to later as ACF+ACD) to prevent particle clotting in ACF plasma during the centrifugation steps. VTCs were then washed 3 times with PBS and suspended in a final volume of 50 μL of detergent solution (0.06 M Tris-HCl, 1% SDS, 10% glycerol, lane marker tracking dye, pH 6.8) obtained from a SDS-PAGE Sample Prep Kit (Pierce). The VTC dispersion was then heated to 95°C for 5 min using a thermocycler to remove the corona proteins and then centrifuged for 5 min to collect the protein supernatant. This is a commonly used approach to remove the corona from particles exposed to plasma or serum [15,26,27]. A reducing agent is optional for this method and was not used here to maintain the full size of proteins in the corona [15,26,27]. For each condition, 15 μL of the protein supernatant was loaded into an individual lane on the gel and ran for ~25 min at 200 V. The molecular weight standard was obtained from Bio-Rad Laboratories, Precision Plus Dual Color Protein Standards.

2.8 Statistical methods

Data was analyzed using Prism. Data in figures was plotted with standard error and comparisons between adhesion assays were performed using 1 way ANOVA with Tukey post-test and confidence interval of 99% (α=0.01). In some instances, an unpaired t-test was employed.

3. Results

3.1 Impact of anticoagulant and its absence on the adhesion efficiency of various VTC materials

Targeted nanoparticles were incubated in the blood medium of interest, citrated plasma, heparinized plasma or serum, for 5 min followed by evaluation of their adhesion efficiency, where particles suspended in whole blood (with either ACD or heparin as the anticoagulant) or RBCs-in-serum are exposed to an activated HUVEC monolayer in a 5 min flow assay. We anticipate that the 5 min of initial exposure to the blood medium is adequate for a stable protein corona to form on nanoparticles, as recent studies report that the nanoparticle plasma protein corona reaches qualitative equilibrium after ~30 sec of plasma exposure time [28,29]. Correspondingly, we observed that maximum reduction in PLGA particle adhesion occurs in as little as 30 sec of particle contact with plasma and was stable up to 5 min (Supplement Figure 2), suggesting that any dynamic processes occurring at later time points contributes a minimal role in orchestrating particle adhesion reduction [3]. Undiluted plasma or plasma product was employed in this work as it best represents the bloodstream condition *in vivo* [23,30,31].

Figure 1 shows the adhesion density of sLe^a-targeted particles of different material types to an activated HUVEC monolayer in flow of different blood mediums relative to the adhesion of the same particles in RBCs-in-VB (control). The adhesion density observed for PLGA and PLA particles at the endothelial wall were 75 to 82% lower in ACD and heparinized WB flows than the adhesion density of the same particles in RBCs-in-VB flows. In contrast, the adhesion density for PS, Si, and PCL particles in ACD WB were only moderately lower relative to the control (< 40% reduction). The use of heparin as anticoagulant in WB resulted in greater than 80% reduction in particle adhesion compared to the control for PS, but Si and PCL showed moderate effects with less than 60% adhesion reduction observed. A significant reduction in adhesion occurred for particles of all material types in RBCs-in-serum flows, where >80% reduction was observed relative to the control. To confirm that the adhesion in blood flows is specific, control experiments were performed with sLe^a-coated PLGA and PS particles in ACD WB flow over a non-activated HUVEC monolayer (no E-selectin expression). Particle adhesion density for PS particles was significantly lower on non-activated HUVEC relative to the adhesion density on activated HUVEC as previously reported (Supplement Figure 3) [23]. However, in the case of PLGA, particle adhesion is low for both non-activated and activated monolayer due to negative adhesion effects of the corona in ACD WB. Overall, the impact of the protein corona on VTC adhesion was magnified in RBCs-in-serum and heparinized WB flows when compared to VTC adhesion in ACD WB for nearly all materials tested.

3.2 Evaluation of HUVEC adhesion of various VTCs in anticoagulant-free WB flow

Particle adhesion in anticoagulant-free (ACF) WB was evaluated in attempt to better mimic the *in vivo* human blood flow environment. The adhesion density of PS, Si, PLGA, and PCL VTCs were ~80% lower in ACF WB flows relative to the buffer control assay while PLA VTCs had a 95% reduction. The observed magnitude of VTC adhesion reduction in ACF WB was similar to observation with VTCs in RBCs-in-Serum (also anticoagulant-free) for

all material types with the exception of PLGA. Instead, PLGA showed improved performance ($P<0.0001$ via two-tailed, unpaired t-test) in ACF blood (~80% reduction) compared to RBCs-in-Serum (~90% reduction). Overall, the absence of anticoagulant in blood (e.g. ACF WB) compared to anticoagulated WB was shown to exert a greater extent of adhesion reduction on particles irrespective of the material type.

3.3 Impact of ligand density in mitigating plasma-associated VTC adhesion reduction

Previous work observed that the density of targeting ligand on VTC surface can play a role in mitigating the extent of the negative impact of the plasma protein corona on the adhesion of PLGA VTCs in ACD treated blood [3]. We explore this possibility here for particle adhesion in all the different blood conditions. As shown in Figure 3, PLGA particles having a high ligand density of ~15,000 sLe^a sites μm^{-2} displayed improved adhesion in ACD WB, exhibiting only 30% reduction relative to the control. In addition, only ~55% adhesion reduction was observed in heparinized WB with the high ligand density. In contrast, increasing the site density of PLGA VTCs did not improve their relative adhesion density in RBC-in-serum or ACF WB flows (compare to Figure 1 and 2). Similarly, having a moderately higher ligand density (~7000 sLe^a sites μm^{-2}) on PCL did not significantly impact their relative adhesion in ACD WB, heparinized WB, or serum (Figure 4). A further increase in PCL site density to ~15,000 sLe^a sites μm^{-2} offered no additional recovery in adhesion for ACD WB (Supplement Figure 4). Overall, the magnitude of the targeting ligand density was observed to abate the negative impact of the protein corona for PLGA in anticoagulated whole blood flows but had no effect on adhesion in RBCs-in-Serum or ACF WB, where anticoagulant was absent.

3.4 Evaluation of differences in VTC plasma protein corona relative to material type and flow medium

We previously reported that the corona formed on PLGA VTCs in ACD blood, when analyzed via SDS-PAGE, contained a higher amount of proteins in the 150 kDa molecular weight range, which were mainly immunoglobulins as determined by mass spectrometry analysis of the corona [3], relative to PS VTCs and that the intensity of this 150 kDa band directly correlated with the extent of the negative impact of plasma proteins on their adhesion efficiency (see Figure 9 in Reference [3]). To determine whether the same large plasma proteins are important in the differential impact of the different blood mediums on VTC adhesion in this work, we conducted an SDS-PAGE analysis of the corona formed on PLGA VTCs incubated in various mediums similar to our prior publication. We then evaluated whether differential protein adsorption also explained the differential impact of plasma on VTCs of different materials via SDS-PAGE analysis of the different VTCs in ACD blood. For this work, VTCs were incubated in the blood medium of choice for 5 min followed by a 5 min centrifugation step. Thus, particles were exposed to the blood medium for a total of 10 min similar to the flow assays.

Figure 5A presents an image of the SDS-PAGE gel for PLGA particles in which there is a notable increase (2.0 +/− 0.4 folds via ImageJ) in the intensity of the band at the 150 kDa mark for the corona acquired from serum versus ACD plasma. However, the adsorption intensity of immunoglobulins and other large proteins is reduced in the corona derived from

heparinized blood-derived, despite the fact that VTCs experienced the same or a larger adhesion reduction in heparin compared to ACD WB flow. It is worth noting that the SDS-PAGE protein profile for a 2% solution of plasma (ACD and Heparin) was mostly similar to the profile obtained for a 2% solution of serum with the exception of the depletion of a relatively high molecular weight band in the free serum profile (Supplement Figure 5; lane 9, > 250 kDa), which is likely fibrinogen based on general knowledge of serum and plasma proteomics [15].

In terms of material type, SDS-PAGE analysis of PLGA, PCL, and PLA coronae formed in ACD WB revealed increased adsorption (1.47 +/− 0.10 folds via ImageJ) of 150 kDa proteins on PLGA and PLA particles relative to PCL (Figure 5B). On the contrary, PCL exhibited increased albumin adsorption (1.55 +/− 0.10 increase in relative intensity) compared to PLGA and PLA particles. Furthermore, SDS-PAGE analysis of PCL particles soaked in ACF plasma showed enhanced adsorption of protein in 150 kDa band compared to ACD soaked particles (Figure 5C). In addition, zeta potential measurements (Supplement Figure 6) were performed for all particle materials soaked in ACD plasma, heparin plasma, serum, and viscous buffer to provide insight into the influence of electrostatic interactions and overall protein content in the various coronae across material types. Minimal differences in zeta potential were observed between the different materials soaked in plasma and serum media. Overall, the increased presence of large proteins in the corona of VTCs correlates with the decrease in particle adhesion in plasma and anticoagulant free blood flows as previously reported [3].

4. Discussion

The data presented in this work demonstrates that the presence of anticoagulant in blood plays a significant role in modulating the adhesion efficiency of VTCs to HUVECs in human blood flow, depending on the VTC material type and ligand density. Specifically, all VTC materials exhibit significantly low flow adhesion (≥ 75% reduction relative to RBCs-in-VB) when a suspension of RBCs-in-Serum or ACF whole blood is used as flow medium, while a generally milder negative effect on particle adhesion is observed in anticoagulant-containing whole blood flows with the exception of PLGA and PLA VTCs. Our observation of significantly reduced particle adhesion in non-anticoagulant-containing blood flows was attributed to increased adsorption of immunoglobulin proteins (~150 kDa), e.g. serum-exposed versus plasma-exposed particles. Between the two anticoagulants evaluated, ACD appears to mute the effect of plasma proteins on VTC adhesion more than heparin, where ACD WB adhesion was reduced only ~35% relative to control for PS, Si, and PCL, while ~60–80% relative reduction was observed in heparinized WB for VTCs of these materials. Increasing the particle ligand density was only effective against adhesion reduction in anticoagulant-containing WB, particularly for ACD WB, where sensitive materials like PLGA recovered up to 70% adhesion relative to buffer. Overall, PLGA and PLA VTCs exhibited the greatest adhesion reduction in anticoagulant-containing blood flows, while PCL and Si VTCs demonstrated distinct resistance to the impact of plasma proteins on their adhesion.

We anticipated that the impact of plasma proteins on VTC adhesion would be more pronounced in serum versus anticoagulant-containing plasma blood flows. Though serum is devoid of several large proteins involved in the clotting process, including fibrinogen, factor V and fibronectin [7,12], immunoglobulins that are the critical "negative" proteins for VTC adhesion are expected to be present in roughly the same concentration between anticoagulant-containing WB and RBCs-in-Serum. Indeed, immunoglobulins such as IgG have been quantified and observed to be highly similar in concentration between human serum and plasma, typically between a range of ~5–20 mg mL^{-1} [32,33]. Thus, it was expected that a more favorable landscape for immunoglobulin adsorption on particles results in the absence of anticoagulant in serum; hence the observed increase in immunoglobulin adsorption (~2-fold increase in intensity) on serum soaked particles (Figure 5) and the downstream stronger negative effect of serum on particle adhesion.

While the negative impact of plasma proteins on VTC adhesion was overall tempered in anticoagulant-containing blood flows, VTCs adhesion was significantly better in WB flows with ACD as the anticoagulant compared to heparin. This observation is not surprising as heparin and ACD anticoagulants act by different mechanisms. Heparin (which acts to prevent coagulation by catalyzing inactivation of thrombin by antithrombin III) binds to a significant number of other plasma proteins [34], and the binding of heparin/heparin sulfate to these "heparin-binding proteins" can modify their activities, metabolism and concentration [17,35]. A study by Kim et al. identified a variety of proteins that are contained in higher concentration in heparin versus citrated plasma, including α2-macroglobulin, haptoglobulin precursor, Apo-AI, Apo J precursor, complement factor H precursor [12]. A recent work by Schöttler et al. also observed slight differences in the protein corona between polystyrene NPs exposed to heparin and citrated blood, where a compositional increase in fibrinogen and decrease in vitronectin was observed in citrate relative to heparin corona, and these particles exhibited differential uptake in HeLa cells and macrophages [14]. Similarly, the corona profiles observed for PLGA particles here show differences between heparin versus ACD exposed particles. The fact that immunoglobulin band previously linked to the low adhesion of PLGA particles in citrated blood is not prominent in the corona of PLGA particles exposed to heparinized blood may suggest that other proteins are involved in causing enhanced adhesion reduction of VTCs in heparin versus citrated blood flow. Notably, the main unique band in the heparin lane (Figure 5A) is between 100 and 150 kDa, possibly a form of haptoglobulin (~100 kDa) or complement factor H (~140 kDa), given the fact these proteins have been identified to be in higher concentration for heparin versus citrated plasma [12]. We will probe this potential impact of other plasma proteins elevated in heparinized blood on VTC adhesion in future studies.

The impact of VTC material type on protein adsorption and particle adhesion also comprised a major component of this work. Overall, PLGA and PLA closely resembled each other and showed a large reduction (>75%) in their blood flow adhesion relative to the control assay in all suspending fluids tested (Figure 1 and 2). In contrast, PCL and Si mimicked each other, both materials exhibiting a mild adhesion reduction in anticoagulant-containing blood relative to the other materials. Interestingly, this impact on particle adhesion of material type was eliminated for non-anticoagulant-containing fluids (i.e. ACF WB and RBCs-in-Serum) with all materials exhibiting a low adhesion density (≤ 75% reduction). Given that the zeta

potential was highly similar for all materials in plasma and serum (Supplement Figure 5), electrostatic interactions likely do not explain the differential adhesion behavior between these materials. Instead, material-dependent VTC adhesion efficiency in ACD WB may be linked to hydrophobicity, since PCL and PS particles (which showed better adhesion efficiency in ACD WB) are of greater hydrophobicity than PLA and PLGA [36]. Furthermore, hydrophobicity is generally known to be an important parameter that affects the formation of a VTC's corona in terms of type and amount of bound proteins [19,37,38]. Hydrophobic particles are known to attract greater amounts of protein in the corona, which might be expected to enhance any corona-induced effect [19]. However, hydrophobic patches also maintain a higher affinity for albumin adsorption, as observed here with PCL particles relative to PLGA and PLA, which has been discussed in the literature to reduce nonspecific protein adsorption on NPs, improve their circulation time, and limit phagocytosis; thus, albumin is considered dysopsonic in nature [19,27,38–42]. Proteins like IgG are opsonic in nature and promote clearance from the bloodstream via macrophage phagocytosis [43]. There is visibly reduced immunoglobulin and increased albumin presence on PCL relative to PLA and PLGA (Figure 5B). Albumin here may act as a positive protein to mitigate the adsorption on PCL VTCs of the large immunoglobulin that were previously linked to reduced adhesion effects in ACD plasma [27]. This innate resistance of PCL to adsorption of immunoglobulin also likely explains the lack of impact of ligand density on adhesion PCL VTCs in anticoagulant-containing blood flows, whereas for PLGA and PLA VTCs that highly attract immunoglobulins in their corona, higher ligand density implies a reduced surface area for protein adsorption (Figure 3, 4). Finally, Si, although a relatively hydrophilic material, may benefit independently due to its higher particle density relative to all other materials studied here, based on previous work showing that particle density improves adhesion in RBCs-in-Buffer flow [4].

It is important to note that the carboxylic acid and avidin surface density will be present as a distribution on the particle surface, which may cause particle-to-particle variation in the corona composition or conformation of adsorbed corona proteins [41,44,45]. To mitigate any potential contribution of batch-to-batch variations linked to the associated particle processing steps, VTC adhesion assays were performed head-to-head for each material type in the different suspending fluids, i.e. same day and same particle batch, and the results normalized to the buffer control. Thus, it is expected that the observed differential VTC adhesion efficiency in the different blood medium for a given material type reported here is largely the result of differential protein affinity for the particle material surface rather than subtle differences in the distributions of carboxylic acid and avidin groups on the particle surface.

Also, we make the distinction here that non-PEG particles were employed in this work despite the fact that PEGylation of particle surfaces is widely used as a strategy to limit protein adsorption to drug carriers, resulting in delayed recognition by the immune system and long circulation time *in vivo* [46]. Non-PEG particles were employed based on multiple considerations. Specifically, recent studies have shown that corona-induced reduction of cell uptake, targeting, and blood flow adhesion persists despite functionalization of particles with intermediate brush to brush-range PEG densities [3,6,47–49]. In addition, recent work from our lab has shown that corona-induced adhesion reduction in porcine blood for 500 nm

diameter polystyrene spheres did not benefit from surface PEGylation [49]. However, a recent report by Dai et al. observe that corona-induced negative effects on cell targeting can be mitigated via the use of refined "backfilling" PEGylation techniques [50]. Despite this highly valuable technique, however, PEGylation has recently been shown to generate an immune response via anti-PEG antibodies upon re-administration, potentially limiting its application *in vivo* [51,52]. As such, several recent studies have focused on identifying alternative approaches to mitigating plasma protein adsorption on biomaterials. Zwitterionic surface coatings, a class of non-fouling, biocompatible materials capable of complete resistance to protein adsorption, are the most promising contender; offering a refined alternative to PEGylation [53]. Zwitterionic materials bind water via electrostatic interactions as opposed to PEG, which exploits H-bonding forces. Given the strength of electrostatic interactions, zwitterionic-induced hydration is much stronger [54], leading to minimal (if any) protein adsorption on surfaces coated with these materials [55]. Poly(sulfobetaine) (pSB) and poly(carboxybetaine) (pCB) are two common types of zwitterionic materials, but pCB is more attractive due to its potential for functionalization with aminated biomolecules via simple carbodiimide chemistry given its free carboxylate groups. Recent studies have observed significant stability of gold pCB NPs in undiluted serum via minimal change in size measured by DLS up to 72 hr, while PEG NPs showed substantial size increases indicating protein fouling [53]. ELISA studies have also shown significant reduction in IgG adsorption on hydrogels containing mixed-charge compounds similar to zwitterions, as opposed to purely positively charged compounds. Thus, coating PLGA and other biodegradable particles with pCB or similar zwitterionic materials may provide a promising new direction for elimination of corona-induced negative adhesion of VTCs in human blood flow.

In addition to exploiting anti-fouling materials, there is growing shift in the literature towards exploiting the corona, rather than eliminate it, for targeting specific cells or cellular function [56,57]. For example, many researchers have explored covalent attachment of albumin and apolipoproteins to the VTC particle surface to direct cell-specific targeting and minimize opsonin adsorption [26,58–60]. This approach may be useful here to prevent corona-induced adhesion reduction of VTCs in light of the high absorption of albumin on PCL VTCs that appear to resist immunoglobulin adsorption. We will explore this and other promising approaches in our future work.

5. Conclusion

This study has revealed that the absence of anticoagulant magnifies the negative impact of the plasma protein corona on VTC adhesion to a model vascular wall *in vitro* via enhanced immunoglobulin adsorption on drug carriers relative to that observed in anticoagulant-containing blood flows. Therefore, it is likely that anticoagulant-containing whole blood may result in an overestimation of drug carrier adhesion efficiency to the vascular wall *in vivo*, given the significantly enhanced negative corona impact on the adhesion of VTCs observed in non-anticoagulant-containing blood flows. In light of our previous work and recently reported failing of PEG coatings, it is likely that alteration in VTC surfaces that lead to altered protein corona via use of dysopsonin proteins to counteract enhanced immunoglobulin adsorption on VTCs or zwitterionic materials that better resist protein

fouling is necessary to improve VTC adhesion efficiency *in vivo*. However, an inherent limitation of this work is in the use of *in vitro* assays with blood outside the body. This system, although a predictive indicator of human blood *in vivo*, likely does not fully capture the landscape for protein adsorption and expected binding efficiency in a clinical setting. Next steps to better predict adhesion efficiency in human would likely involve *in vivo* evaluation of drug carriers in a porcine model, as we have previously identified this species to be a suitable comparison to human with regard to corona-associated adhesion effects.

Supplementary Material

Refer to Web version on PubMed Central for supplementary material.

Acknowledgments

This work was supported by the National Institute of Health [grant number R01 HL115138] to OE-A; and the Cellular Biotechnology Training Program [grant number T32GM008353] to DJ Sobczynski. The authors would like to thank Professors Thurber and Wen for helpful discussions about protein analysis.

References

1. Psarros C, Lee R, Margaritis M, Antoniades C. Nanomedicine for the prevention, treatment and imaging of atherosclerosis. Maturitas. 2012; 73:52–60. [PubMed: 22261366]
2. Hajitou A, Pasqualini R, Arap W. Vascular targeting: recent advances and therapeutic perspectives. Trends Cardiovasc Med. 2006; 16:80–88. [PubMed: 16546688]
3. Sobczynski DJ, Charoenphol P, Heslinga MJ, Onyskiw PJ, Namdee K, Thompson AJ, Eniola-Adefeso O. Plasma protein corona modulates the vascular wall interaction of drug carriers in a material and donor specific manner. PLoS One. 2014; 9:e107408. [PubMed: 25229244]
4. Thompson AJ, Eniola-Adefeso O. Dense nanoparticles exhibit enhanced vascular wall targeting over neutrally buoyant nanoparticles in human blood flow. Acta Biomater. 2015; 21:99–108. [PubMed: 25870170]
5. Namdee K, Sobczynski DJ, Onyskiw PJ, Eniola-Adefeso O. Differential Impact of Plasma Proteins on the Adhesion Efficiency of Vascular-Targeted Carriers (VTCs) in Blood of Common Laboratory Animals. Bioconjug Chem. 2015; 26:2419–2428. [PubMed: 26505780]
6. Salvati A, Pitek AS, Monopoli MP, Prapainop K, Bombelli FB, Hristov DR, Kelly PM, Aberg C, Mahon E, Dawson KA. Transferrin-functionalized nanoparticles lose their targeting capabilities when a biomolecule corona adsorbs on the surface. Nat Nanotechnol. 2013; 8:137–143. [PubMed: 23334168]
7. Ayache S, Panelli MC, Byrne KM, Slezak S, Leitman SF, Marincola FM, Stroncek DF. Comparison of proteomic profiles of serum, plasma, and modified media supplements used for cell culture and expansion. J Transl Med. 2006; 4:40. [PubMed: 17020621]
8. Tammen H, Schulte I, Hess R, Menzel C, Kellmann M, Mohring T, Schulz-Knappe P. Peptidomic analysis of human blood specimens: Comparison between plasma specimens and serum by differential peptide display. Proteomics. 2005; 5:3414–3422. [PubMed: 16038021]
9. Müller, RH.; Göppert, TM. Role of Lipid Excipients in Modifying Oral and Parenteral Drug Delivery: Basic Principles and Biological Examples. John Wiley & Sons; 2007.
10. Mirshafiee V, Mahmoudi M, Lou K, Cheng J, Kraft ML. Protein corona significantly reduces active targeting yield. Chem Commun (Camb). 2013; 49:2557–2559. [PubMed: 23423192]
11. Monopoli MP, Walczyk D, Campbell A, Elia G, Lynch I, Baldelli Bombelli F, Dawson KA. Physical-Chemical aspects of protein corona: Relevance to in vitro and in vivo biological impacts of nanoparticles. J Am Chem Soc. 2011; 133:2525–2534. [PubMed: 21288025]
12. Kim HJ, Kim MR, So EJ, Kim CW. Comparison of proteomes in various human plasma preparations by two-dimensional gel electrophoresis. J Biochem Biophys Methods. 2007; 70:619–625. [PubMed: 17368557]

13. Issaq HJ, Xiao Z, Veenstra TD. Serum and plasma proteomics. Chem Rev. 2007; 107:3601–3620. [PubMed: 17636887]
14. Schöttler S, Klein K, Landfester K, Mailänder V. Protein source and choice of anticoagulant decisively affect nanoparticle protein corona and cellular uptake. Nanoscale. 2015; 00:1–3.
15. Mirshafiee V, Kim R, Mahmoudi M, Kraft ML. The importance of selecting a proper biological milieu for protein corona analysis in vitro: human plasma vs. human serum. Int J Biochem Cell Biol. 2016; 75:188–195. [PubMed: 26643610]
16. Killeen R, Wait R, Begum S, Gray E, Mulloy B. Identification of major heparin-binding proteins in plasma using electrophoresis and mass spectrometry. Int J Exp Pathol. 2004; 85:A69–A69.
17. Conrad, E. Heparin-binding proteins. Academic Press; 1997.
18. Capila I, Linhardt RJ. Heparin-protein interactions. Angew Chem Int Ed Engl. 2002; 41:391–412. [PubMed: 12491369]
19. Rahman, M.; Laurent, S.; Tawil, N.; Yahia, LH.; Mahmoudi, M. Protein-Nanoparticle Interactions. Springer; Berlin Heidelberg: 2013.
20. Deng ZJ, Mortimer G, Schiller T, Musumeci A, Martin D, Minchin RF. Differential plasma protein binding to metal oxide nanoparticles. Nanotechnology. 2009; 20:455101. [PubMed: 19822937]
21. Banfi G, Salvagno GL, Lippi G. The role of ethylenediamine tetraacetic acid (EDTA) as in vitro anticoagulant for diagnostic purposes. Clin Chem Lab Med. 2007; 45:565–576. [PubMed: 17484616]
22. McCafferty MH, Lepow M, Saba TM, Cho E, Meuwissen H, White J, Zuckerbrod SF. Normal fibronectin levels as a function of age in the pediatric population. Pediatr Res. 1983; 17:482–485. [PubMed: 6877901]
23. Charoenphol P, Huang RB, Eniola-Adefeso O. Potential role of size and hemodynamics in the efficacy of vascular-targeted spherical drug carriers. Biomaterials. 2010; 31:1392–1402. [PubMed: 19954839]
24. Huang RB, Eniola-Adefeso O. Shear stress modulation of IL-1β-induced E-selectin expression in human endothelial cells. PLoS One. 2012; 7:1–9.
25. Huang RB, Gonzalez AL, Eniola-Adefeso O. Laminar shear stress elicit distinct endothelial cell e-selectin expression pattern via TNFα and IL-1β activation. Biotechnol Bioeng. 2013; 110:999–1003. [PubMed: 23055258]
26. Mirshafiee V, Kim R, Park S, Mahmoudi M, Kraft ML. Impact of protein pre-coating on the protein corona composition and nanoparticle cellular uptake. Biomaterials. 2016; 75:295–304. [PubMed: 26513421]
27. Tenzer S, Docter D, Rosfa S, Wlodarski A, Kuharev J, Rekik A, Knauer SK, Bantz C, Nawroth T, Bier C, Sirirattanapan J, Mann W, Treuel L, Zellner R, Maskos M, Schild H, Stauber RH. Nanoparticle size is a critical physicochemical determinant of the human blood plasma corona: A comprehensive quantitative proteomic analysis. ACS Nano. 2011; 5:7155–7167. [PubMed: 21866933]
28. Tenzer S, Docter D, Kuharev J, Musyanovych A, Fetz V, Hecht R, Schlenk F, Fischer D, Kiouptsi K, Reinhardt C, Landfester K, Schild H, Maskos M, Knauer SK, Stauber RH. Rapid formation of plasma protein corona critically affects nanoparticle pathophysiology. Nat Nanotechnol. 2013; 8:772–781. [PubMed: 24056901]
29. Dell'Orco D, Lundqvist M, Oslakovic C, Cedervall T, Linse S. Modeling the time evolution of the nanoparticle-protein corona in a body fluid. PLoS One. 2010; 5:e10949. [PubMed: 20532175]
30. Charoenphol P, Mocherla S, Bouis D, Namdee K, Pinsky DJ, Eniola-Adefeso O. Targeting therapeutics to the vascular wall in atherosclerosis--carrier size matters. Atherosclerosis. 2011; 217:364–370. [PubMed: 21601207]
31. Müller K, Fedosov Da, Gompper G. Margination of micro- and nano-particles in blood flow and its effect on drug delivery. Sci Rep. 2014; 4:4871. [PubMed: 24786000]
32. Gonzalez-Quintela A, Alende R, Gude F, Campos J, Rey J, Meijide LM, Fernandez-Merino C, Vidal C. Serum levels of immunoglobulins (IgG, IgA, IgM) in a general adult population and their relationship with alcohol consumption, smoking and common metabolic abnormalities. Clin Exp Immunol. 2008; 151:42–50. [PubMed: 18005364]

33. Greenough C, Jenkins RE, Kitteringham NR, Pirmohamed M, Park BK, Pennington SR. A method for the rapid depletion of albumin and immunoglobulin from human plasma. Proteomics. 2004; 4:3107–3111. [PubMed: 15378708]
34. Banks RE, Stanley AJ, Cairns DA, Barrett JH, Clarke P, Thompson D, Selby PJ. Influences of blood sample processing on low-molecular-weight proteome identified by surface-enhanced laser desorption/ionization mass spectrometry. Clin Chem. 2005; 51:1637–1649. [PubMed: 16002455]
35. Thacker BE, Xu D, Lawrence R, Esko JD. Heparan sulfate 3-O-sulfation: A rare modification in search of a function. Matrix Biol. 2014; 35:60–72. [PubMed: 24361527]
36. D'Addio SM, Saad W, Ansell SM, Squiers JJ, Adamson DH, Herrera-Alonso M, Wohl AR, Hoye TR, Macosko CW, Mayer LD, Vauthier C, Prud'homme RK. Effects of block copolymer properties on nanocarrier protection from in vivo clearance. J Control Release. 2012; 162:208–217. [PubMed: 22732478]
37. Gessner A, Waicz R, Lieske A, Paulke B, Ma K. Nanoparticles with decreasing surface hydrophobicities: influence on plasma protein adsorption. Int J Pharm. 2000; 196:245–249. [PubMed: 10699728]
38. Aggarwal P, Hall JB, McLeland CB, Dobrovolskaia Ma, McNeil SE. Nanoparticle interaction with plasma proteins as it relates to particle biodistribution, biocompatibility and therapeutic efficacy. Adv Drug Deliv Rev. 2009; 61:428–437. [PubMed: 19376175]
39. Caracciolo G, Pozzi D, Capriotti AL, Cavaliere C, Laganà A. Effect of DOPE and cholesterol on the protein adsorption onto lipid nanoparticles. J Nanoparticle Res. 2013; 15:1498.
40. Gref R, Lück M, Quellec P. "Stealth"corona-core nanoparticles surface modified by polyethylene glycol (PEG): influences of the corona (PEG chain length and surface density) and of the core. Colloids Surfaces B Biointerfaces. 2000; 18:301–313. [PubMed: 10915952]
41. Pearson RM, Juettner VV, Hong S. Biomolecular corona on nanoparticles: a survey of recent literature and its implications in targeted drug delivery. Front Chem. 2014; 2
42. Staufenbiel S, Weise C, Müller RH. Targeting of Intravenous Polymeric Nanoparticles by Differential Protein Adsorption. Macromol Symp. 2014; 345:42–50.
43. Mahon E, Salvati A, Bombelli FB, Lynch I, Dawson KA. Designing the nanoparticle – biomolecule interface for " targeting and therapeutic delivery". J Control Release. 2012; 161:164–174. [PubMed: 22516097]
44. Sobczynski DJ, Fish MB, Fromen CA, Carasco-Teja M, Coleman RM, Eniola-Adefeso O. Drug carrier interaction with blood: a critical aspect for high-efficient vascular-targeted drug delivery systems. Ther Deliv. 2015; 6:915–934. [PubMed: 26272334]
45. Lundqvist M, Stigler J, Elia G, Lynch I, Cedervall T, Dawson KA. Nanoparticle size and surface properties determine the protein corona with possible implications for biological impacts. Proc Natl Acad Sci. 2008; 105:14265–14270. [PubMed: 18809927]
46. Owens DE, Peppas NA. Opsonization, biodistribution, and pharmacokinetics of polymeric nanoparticles. Int J Pharm. 2006; 307:93–102. [PubMed: 16303268]
47. Kang B, Okwieka P, Schöttler S, Winzen S, Langhanki J, Mohr K, Opatz T, Mailander V, Landfester K, Wurm FR. Carbohydrate-Based Nanocarriers Exhibiting Specific Cell Targeting with Minimum Influence from the Protein Corona. Angew Chem Int Ed Engl. 2015; 54:7436–7440. [PubMed: 25940402]
48. Wattendorf U, Merkle HP. PEGylation as a tool for the biomedical engineering of surface modified microparticles. J Pharm Sci. 2008; 97:4655–4669. [PubMed: 18306270]
49. Namdee K, Sobczynski DJ, Onyskiw PJ, Eniola-Adefeso O. Differential Impact of Plasma Proteins on the Adhesion Efficiency of Vascular-Targeted Carriers (VTCs) in Blood of Common Laboratory Animals. Bioconjug Chem. 2015; 26:2419–2428. [PubMed: 26505780]
50. Dai Q, Walkey C, Chan WCW. Polyethylene glycol backfilling mitigates the negative impact of the protein corona on nanoparticle cell targeting. Angew Chem Int Ed Engl. 2014; 53:5093–5096. [PubMed: 24700480]
51. Howard M, Zern BJ, Anselmo AC, Shuvaev VV, Mitragotri S, Muzykantov V. Vascular Targeting of Nanocarriers: Perplexing Aspects of the Seemingly Straightforward Paradigm. ACS Nano. 2014; 8:4100–4132. [PubMed: 24787360]

52. Ishida T, Wang X, Shimizu T, Nawata K, Kiwada H. PEGylated liposomes elicit an anti-PEG IgM response in a T cell-independent manner. J Control Release. 2007; 122:349–355. [PubMed: 17610982]
53. Jiang S, Cao Z. Ultralow-fouling, functionalizable, and hydrolyzable zwitterionic materials and their derivatives for biological applications. Adv Mater. 2010; 22:920–932. [PubMed: 20217815]
54. Moyano DF, Saha K, Prakash G, Yan B, Kong H, Yazdani M, Rotello VM. Fabrication of Corona-Free Nanoparticles with Tunable Hydrophobicity. ACS Nano. 2014; 8:6748–6755. [PubMed: 24971670]
55. Yang W, Bai T, Carr LR, Keefe AJ, Xu J, Xue H, Irvin CA, Chen S, Wang J, Jiang S. The effect of lightly crosslinked poly(carboxybetaine) hydrogel coating on the performance of sensors in whole blood. Biomaterials. 2012; 33:7945–7951. [PubMed: 22863377]
56. Caracciolo G, Pozzi D, Capriotti AL, Cavaliere C, Cardarelli F, Bifone A, Lagana A. Cancer cell targeting of lipid gene vectors by protein corona. Nanotech 2012. 2012; 3:354–357.
57. Kreuter J. Nanoparticulate systems for brain delivery of drugs. Adv Drug Deliv Rev. 2001; 47:65–81. [PubMed: 11251246]
58. Kreuter J, Hekmatara T, Dreis S, Vogel T, Gelperina S, Langer K. Covalent attachment of apolipoprotein A-I and apolipoprotein B-100 to albumin nanoparticles enables drug transport into the brain. J Control Release. 2007; 118:54–8. [PubMed: 17250920]
59. Kreuter J, Shamenkov D, Petrov V, Ramge P, Cychutek K, Koch-Brandt C, Alyautdin R. Apolipoprotein-mediated transport of nanoparticle-bound drugs across the blood-brain barrier. J Drug Target. 2002; 10:317–325. [PubMed: 12164380]
60. Michaelis K, Hoffmann MM, Dreis S, Herbert E, Alyautdin RN, Michaelis M, Kreuter J, Langer K. Covalent Linkage of Apolipoprotein E to Albumin Nanoparticles Strongly Enhances Drug Transport into the Brain. J Pharmacol Exp Ther. 2006; 317:1246–1253. [PubMed: 16554356]

Appendix: Supplementary Data

Supplementary data associated with this article is available with the online version.

Statement of Significance

This study addresses the impact of anticoagulant on altering the extent of the previously observed protein corona-induced adhesion reduction of vascular-targeted drug carriers in human blood flows. Specifically, serum blood flow (no anticoagulant) magnifies the negative effect of the plasma protein corona on drug carrier adhesion relative to citrated or heparinized blood flows. Overall, the results from this work suggest that serum better predicts targeted drug carrier adhesion efficiency *in vivo* compared to anti-coagulant-containing plasma. Furthermore, this study offers critical insight into the importance of how the choice of anticoagulant can greatly affect drug delivery-related processes in vitro.

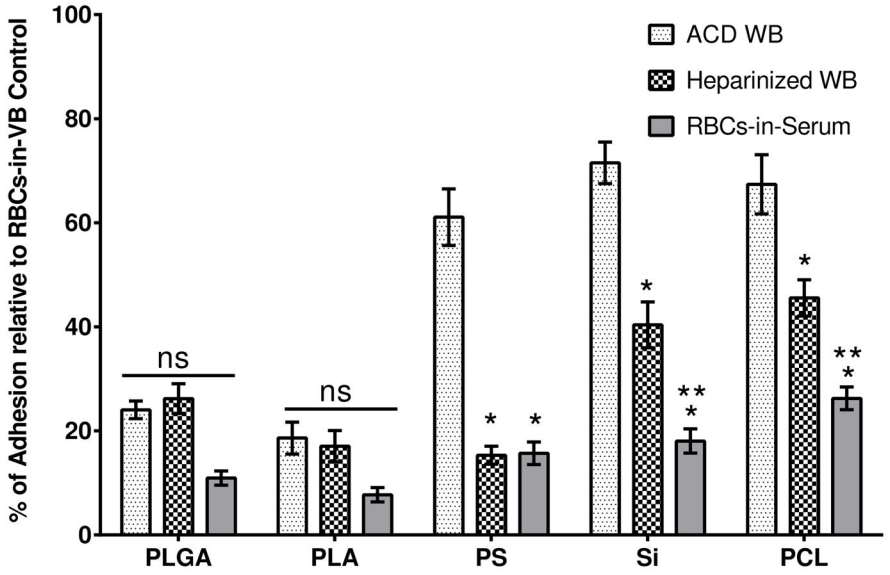

Figure 1.

PPFC assay with VTCs in various anticoagulants: HUVEC adhesion (% relative to RBCs-in-VB Control) for PLGA, PLA, PS, Si, and PCL VTCs in ACD WB, heparinized WB, and RBCs-in-Serum relative to RBCs-in-VB after 5 min of flow at a shear rate of $200s^{-1}$. Particle concentration was fixed to 1 x 10^6 particles mL^{-1}. $n \geq 4$. * = $p<0.01$ relative to ACD-WB trial for given material via one-way ANOVA with Tukey post-test. ** = $p<0.01$ relative to heparinized WB trial for given material via one-way ANOVA with Tukey post-test.

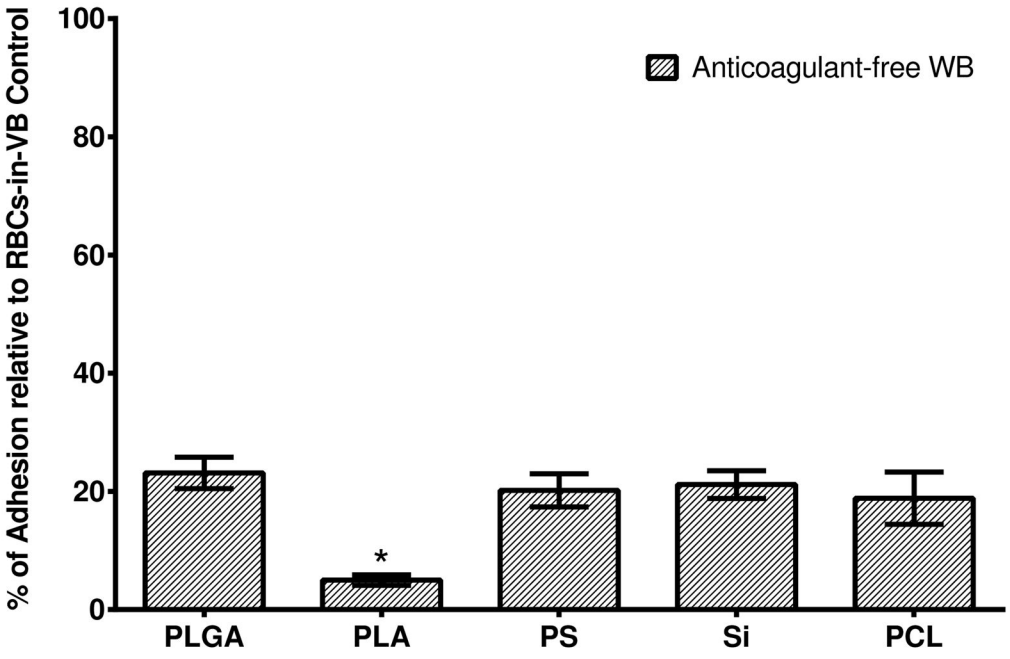

Figure 2.

PPFC assay with VTCs in ACF WB: HUVEC adhesion (% relative to RBCs-in-VB Control) for PLGA, PLA, PS, Si, and PCL VTCs in Anticoagulant-free WB relative to RBCs-in-VB after 5 min of flow at a shear rate of $200s^{-1}$. Particle concentration was fixed to 1×10^6 particles mL^{-1}. $n \geq 3$. * = $p<0.01$ relative to Anticoagulant-free WB trials relative to all other VTC materials.

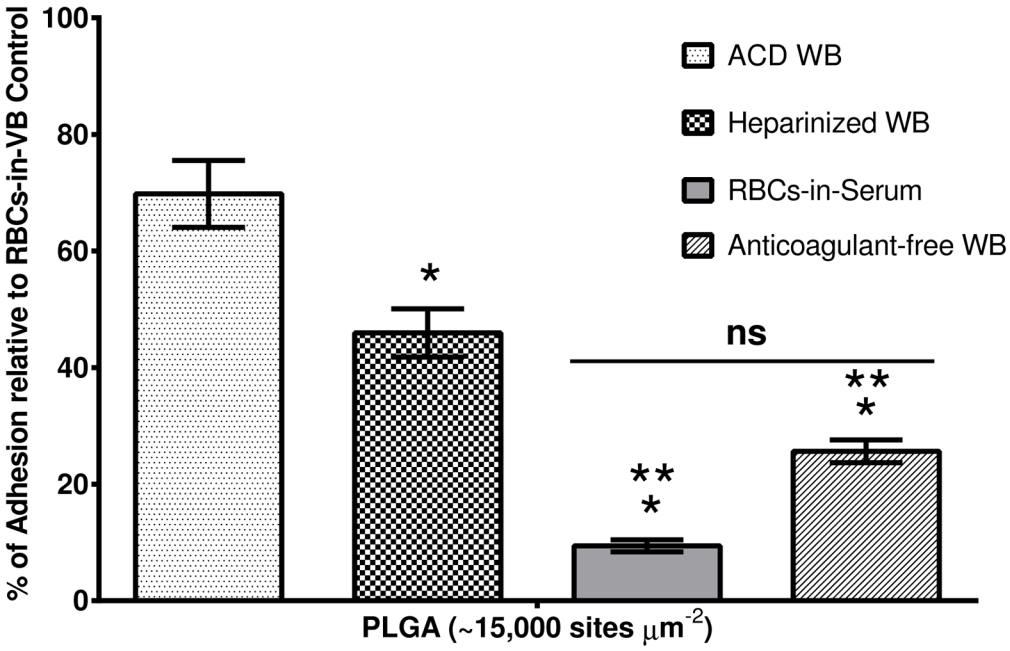

Figure 3.

PPFC assay with high ligand density PLGA VTCs: HUVEC adhesion (% relative to RBCs-in-VB Control) for high ligand density PLGA VTCs (~15,000 sites/μm^2) in ACD WB, heparinized WB, RBCs-in-Serum, and Anticoagulant-free WB after 5 min of flow at a shear rate of $200s^{-1}$. Particle concentration was fixed to 1 x 10^6 particles mL^{-1}. $n \geq 4$. * = $p<0.01$ relative to ACD-WB trial via one-way ANOVA with Tukey post-test. ** = $p<0.01$ relative to heparinized WB trial via one-way ANOVA with Tukey post-test.

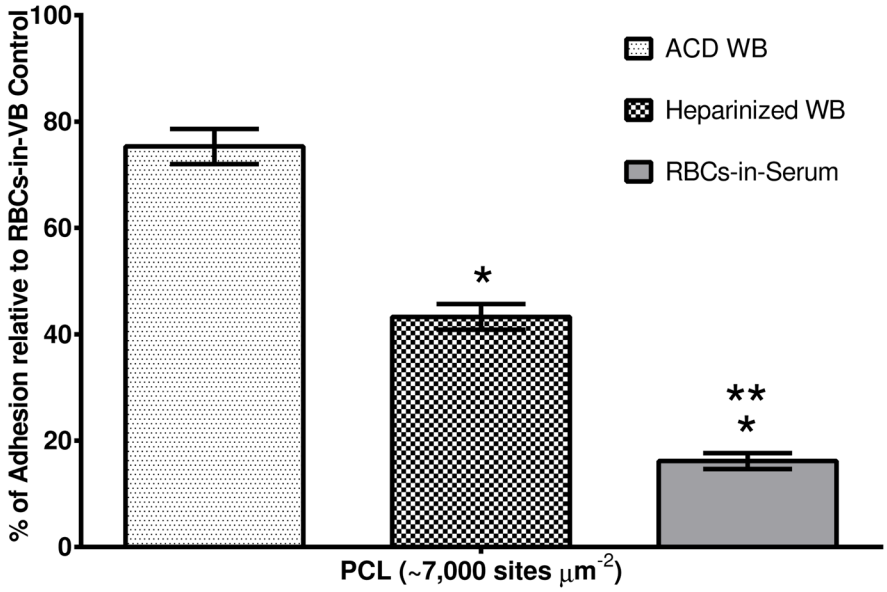

Figure 4.

PPFC assay with high ligand density PCL VTCs: HUVEC adhesion (% relative to RBCs-in-VB Control) for high ligand density PCL VTCs (~7,000 sites/μm^2) in ACD WB, heparinized WB, and RBCs-in-Serum after 5 min of flow at a shear rate of $200 s^{-1}$. Particle concentration was fixed to 1 x 10^6 particles mL^{-1}. $n \geq 4$. * = $p<0.01$ relative to ACD-WB trial via one-way ANOVA with Tukey post-test. ** = $p<0.01$ relative to heparinized WB trial via one-way ANOVA with Tukey post-test.

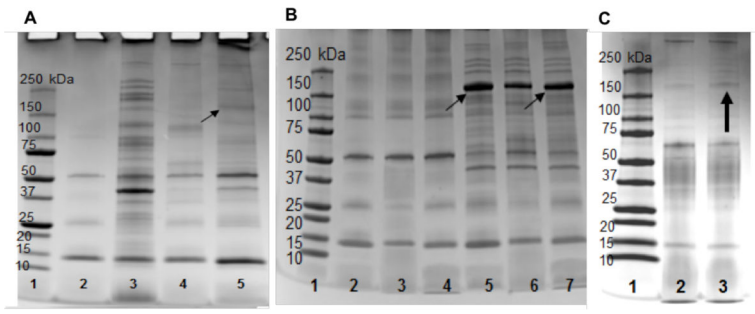

Figure 5.

SDS-PAGE: Characterization of surface bound protein coronae formed on PLGA, PCL, and PLA VTCs exposed to VB, plasma (ACD, heparin), and serum. A) PLGA only, Lane 1: molecular weight standard, Lane 2: corona from VB soak, Lane 3: corona from ACD plasma soak, Lane 4: corona from heparinized plasma soak, Lane 5: corona from serum soak. B) PLGA, PCL, and PLA, Lane 1: molecular weight standard, Lane 2: PLGA corona from VB soak, Lane 3: PCL corona from VB soak, Lane 4: PLA corona from VB soak, Lane 5: PLGA corona from ACD plasma soak, Lane 6: PCL corona from ACD plasma soak, Lane 7: PLA corona from ACD plasma soak. C) ACD (Lane 2) and ACF + ACD (Lane 3) soaked PCL particles

Table 1

VTC DLS sizing measurements

The average VTC diameter (Z-average) and polydispersity index (PDI) is listed for all materials studied here. Data was obtained via DLS using a Malvern Zetasizer Nano equipped with a back scattering detector.		
Material	***Z-Average (nm)***	***PDI***
PLA	635	0.25
PLGA	428	0.18
Si	712	0.12
PS	529	0.12
PCL	600	0.27

Table 2

VTC ligand density quantification

The average sLe^a ligand density per μm^2 and standard error (S.E) is listed for all materials studied here. Data was obtained via flow cytometry (Attune, Applied Biosystems). sLe^a ligand densities were quantified by use of Quantum™ MESF PE calibration beads (Bangs Laboratories)		
Material	***sLe^a density (sites μm^{-2})***	***S.E.***
PLA, PLGA	3500	700
PLGA (“high”)	15300	900
Si	4400	200
PS	6000	300
PCL	2200	500
PCL (“moderate”)	7100	1200
PCL (“high”)	14500	700